

Accumulation of amyloid beta in human glioblastomas

A. Zayas-Santiago ^{*},
A. Díaz-García ^{*},
R. Nuñez-Rodríguez[†] and
M. Inyushin ^{*}

^{*}Physiology Department, Medical School, Universidad Central del Caribe, Puerto Rico, and [†]Biochemistry Department, Medical School, Universidad Central del Caribe, Bayamon

Accepted for publication 2 July 2020

Correspondence: M. Inyushin, Physiology Department, UCC Medical School, Avenue Laurel, Santa Juanita, Bayamon, Puerto Rico 00956.

E-mail: mikhail.inyushin@uccaribe.edu

Summary

Many cancer types are intrinsically associated with specific types of amyloidosis, in which amyloid is accumulated locally inside tumors or systemically. Usually, this condition relates to the hyperproduction of specific amylogenic proteins. Recently, we found that the accumulation of amyloid beta (A β) peptide immunofluorescence is linked to glioma cells in mouse tumors. Here we report that amyloid-specific histochemical dyes reveal amyloid accumulation in all human glioma samples. Application of two different antibodies against A β peptide (a polyclonal antibody against human A β 1–42 and a monoclonal pan-specific mAb-2 antibody against A β) showed that the amyloid in glioma samples contains A β . Amyloid was linked to glioma cells expressing glial-specific fibrillary acidic protein (GFAP) and to glioma blood vessels. Astrocytes close to the glioma site and to affected vessels also accumulated A β . We discuss whether amyloid is produced by glioma cells or is the result of systemic production of A β in response to glioma development due to an innate immunity reaction. We conclude that amyloid build-up in glioma tumors is a part of the tumor environment, and may be used as a target for developing a novel class of anti-tumor drugs and as an antigen for glioma visualization.

Keywords: brain, cancer, human, microscopy, tumor immunology

Introduction

A build-up of amyloid has been reported in many cancerous tumors, and some cancers are intrinsically connected with specific types of amyloidosis. For example, multiple myeloma, as well as malignant lymphoproliferative diseases, such as chronic lymphocytic leukemia, hairy cell leukemia, Hodgkin lymphoma and Waldenstrom's disease, is associated with the hypersecretion of Bence Jones [free immunoglobulin (Ig) light chain] protein, generating a particular form of systemic amyloid light-chain (AL) amyloidosis [1–4]. Unlike systemic amyloidosis, breast cancer exhibits localized light-chain amyloidosis, with amyloid bodies limited to the inside of the tumor [5,6]. Many carcinomas have stroma containing AL-type amyloid [7,8]. Localized AL-type amyloidosis was also found in early-stage non-small-cell adenocarcinomas in kidney and lung [9]. It is important to mention that localized AL amyloidosis is related to many cancer types forming amyloid tumors – the

condition known as amyloid tumor disease. Such local amyloid deposition may be explained by over-expression of the receptors for amyloid protein oligomers. For example, amyloid accumulation in lung cancer is a consequence of the binding of amyloid oligomers to over-expressed amyloid-binding receptor for advanced glycation end products (RAGE) receptors present in lung tumors [10]. However, AL-type amyloid is not the only amyloid found in tumors, and these others are probably of mixed type, as is common for other amyloid diseases, such as Alzheimer's disease (AD) [11]. Many proteins form fibrous aggregates due to cross- β polymerization of β -pleated sheets and co-aggregate with other proteins at elevated concentrations, forming a mixed misfolded amyloid [12,13]. An additional systemic amyloidogenic protein (besides light chain protein) involved in multiple myeloma (and in some other cancers) is β 2-microglobulin (β 2M), an anti-microbial protein with anti-bacterial activity and a light chain of the major histocompatibility complex. β 2M protein hyperproduction is so common

in many cancers (while reduced in gliomas) that it can be used as a tumor marker [14]. These proteins are produced systemically and may accumulate systemically or locally. Conversely, some tissue-specific cancerous tumor types overproduce tissue-specific, aggregation-prone proteins. For example, the amyloid in odontogenic tumors is immunopositive for the enamel matrix protein ameloblastin [15–17]. Unlike odontogenic tumors, the tumoral amyloidosis of bone is usually of β 2M origin and almost always progresses to multiple myeloma [18].

There is another systemic protein that has a β -pleated sheet structure and is prone to aggregation: the amyloid beta ($A\beta$) peptide. While many cells produce $A\beta$, in amyloidosis it usually accumulates in specific tissues. $A\beta$ is a major component of amyloid deposition in AD, in brain trauma (brain tissue), glaucoma (retina), pre-eclampsia (placenta) and many other health conditions and has anti-microbial activity, which may be related to innate immunity (see review: [19,20]). $A\beta$ is known to be elevated in many cancers. For example, the plasma levels of $A\beta$ peptides in esophageal cancer, colorectal cancer, kidney cancer, hepatic cancer and lung cancer patients were significantly higher than in normal controls [21].

It has also been shown that gliomas are extensively infiltrated by platelets [22,23], which are the main source of $A\beta$ in the blood [20,24,25]. These small, anuclear blood cells and their $A\beta$ -containing microvesicles easily penetrate the blood–brain barrier, especially in the glioma-affected zone [22,26,27]. As an important part of innate immunity, platelets respond to bacterial invasions and malignant cancers releasing many factors necessary to recruit other immune cells, but also releasing their own defense peptides, including $A\beta$ [28,29]. The anti-tumor effects of $A\beta$ peptides are well known [30,31], and recently we found an accumulation of $A\beta$ on the surface of glioma cells within glioma tumors in mice. Visible $A\beta$ immunofluorescence in nearby vessels suggests that the most possible source of $A\beta$ in mouse tumor is blood, and we propose that this amyloid build-up could be a target for developing a novel class of drugs for glioma visualization and treatment [32]. The question then is: do human glioma tumors also accumulate amyloid and have $A\beta$ present within the tumor?

Here we report the accumulation of amyloid in human glioma, showing that amyloid is linked to glioma cells of glial origin, both intra- and extracellularly, and to glioma blood vessels. In this study we used various dyes known for specific amyloid staining to visualize amyloid in tumors from surgically removed brain tissue from patients of different ages diagnosed with glioblastoma. Immunostaining revealed that the amyloid in these tumors contains $A\beta$. We also used double immunostaining against human $A\beta$ and specific co-staining of different cell types, as we found that, as well as extracellular deposition of amyloid, many

cells in glioma specifically accumulate this substance. This double staining allowed us to determine which cells in glioma accumulate $A\beta$.

Material and methods

Paraformaldehyde-fixed human glioma tissue samples were obtained with patient consent from collaborators at the Universidad Central del Caribe for future use as unidentifiable tissue samples, as approved by the Institutional Review Board (IRB) Human Research Subject Protection Office (protocol no. 2012-12B). In total, we analyzed glioblastoma samples from five patients.

Tissue preparation and cryosectioning

The tissue was fixed in a solution of 4% paraformaldehyde and incubated overnight (16–24 h) in the same fixative solution. After incubation, the tissue was transferred to phosphate-buffered saline (PBS: NaCl, 137 mM; KCl, 2.70 mM; Na_2HPO_4 , 1.77 mM; pH 7.4). After rinsing the tissue three times for 10 min per rinse at room temperature (RT) in PBS with 5% sucrose (with gentle rotation), the samples were cryoprotected with increasing concentrations of sucrose in PBS, which were obtained by mixing 5% sucrose and 20% sucrose at ratios of 2 : 1, 1 : 1 and 1 : 2. The tissue was incubated for 30 min at each step in the ascending series of sucrose solutions at RT and then finally placed in 20% sucrose at 4°C, allowing preservation of the tissue over a long period. Before staining, 30- μ m slides were prepared from the samples using a cryomicrotome (CM 1850; Leica Microsystems GmbH, Wetzlar, Germany) at -23°C .

Immunostaining, histochemistry and fluorescence confocal microscopy

The slides were air-dried for 30 min and immunostained using a protocol previously established in our laboratory. First, sections were treated for 20 min with a permeabilization solution consisting of 0.03% Triton X-100 and 1% dimethyl sulfoxide (DMSO; MP Biomedicals, Santa Ana, CA, USA) in PBS under gentle agitation on an orbital shaker. Secondly, the sections were treated for 60 min with a blocking solution containing 5% normal goat serum, 5% normal horse serum (Vector Laboratories, Burlingame, CA, USA) and 2% w/v bovine serum albumin (BSA; Sigma-Aldrich, St Louis, MO, USA) in permeabilization solution. Following the blocking step, the sections were processed separately using two different antibodies against $A\beta$. Slices were incubated with a mouse monoclonal antibody against glial fibrillary acidic protein-cyanin 3 (GFAP-Cy3) (1 : 200; Abcam, Cambridge, MA, USA, cat. no. ab49874), a rabbit polyclonal antibody against $A\beta$ 1–42 (1 : 100; Abcam, cat. no. ab216504), a rabbit monoclonal antibody against neuronal

hexaribonucleotide binding protein3 (NeuN)-Alexa Fluor 647 (1 : 100; Abcam, cat. no. ab190565) and a mouse monoclonal antibody (mAb-2) against A β (1 : 100; Abcam, cat. no. 126649), all incubated overnight at 4°C. After three washes with permeabilization solution for 10 min, the secondary antibodies (fluorescein-labeled goat anti-rabbit IgG and fluorescein-labeled horse anti-mouse IgG) were added at a dilution of 1 : 200 with shaking for 2 h at room temperature and protected from light. The slices were then washed three times with PBS for 10 min and once with distilled water before being transferred onto a glass slide containing Fluoroshield mounting medium (Sigma-Aldrich, cat. no. F6057) with 4',6-diamidino-2-phenylindole (DAPI).

For thioflavin staining we used thioflavin S (Th-S). Human brain slices (30 μ m) containing tumors were completely air-dried prior to staining. The slides were first washed with 70% ethyl alcohol (EtOH) for 1 min, followed by 80% EtOH for 1 min, and then incubated for 15 min in a filtered solution of Th-S (0.2- μ m filter). A solution of 1% Th-S was prepared in 80% EtOH. After incubation, the slides were washed with 80% EtOH for 1 min followed by 70% EtOH for 1 min, washed twice with distilled water and air-dried again. The coverslip was mounted with a drop of Vectashield[®] mounting medium for visualization of fluorescence (Vector Laboratories, Burlingame, CA, USA, cat. no. H-1000).

Brilliant blue (BBG) staining was performed as follows. The human brain slices (30 μ m)-containing tumors were allowed to air-dry completely, stained with a drop of 0.25 mg/ml BBG in distilled water (0.2- μ m filter) for 5 min, washed twice with distilled water, and air-dried again. The glass slides were mounted with Fluoroshield mounting medium containing DAPI (Sigma-Aldrich, cat. no. F6057).

Congo red staining was performed as follows. A 0.5% Congo red solution was prepared in 50% alcohol. Human brain slices (30 μ m) containing tumors were air-dried completely, then washed twice with absolute alcohol for 2 min. The slices were then washed with 90% alcohol for 2 min, followed by 70% alcohol for 2 min, washed once with running water for 2 min and incubated for 20 min in a filtered solution of Congo red (0.2- μ m filter). After incubation, the slides were rinsed with distilled water once, rinsed repeatedly in alkaline alcohol solution (five to 10 times), and rinsed in tap water for 2 min. Finally, the slices were dehydrated through immersion in 95% alcohol, followed by two immersions in 100% alcohol for 3 min each. The glass slides were mounted with Fluoroshield mounting medium containing DAPI.

Fluorescein isothiocyanate (FITC) excitation/emission filters were used to visualize specific amyloid-associated Th-S and Congo red fluorescence, whereas tetramethylrhodamine isothiocyanate (TRITC) filters were used to reveal non-specific Congo red fluorescence, and TRITC

excitation/emission filters were used to visualize BBG fluorescence.

Images were acquired using an Olympus Fluoview FV1000 scanning inverted confocal microscope system equipped with a 4 \times , 10 \times , 20 \times or 40 \times /1.43 oil objective (Olympus, Melville, NY, USA). The images were analyzed using ImageJ software (version 1.8.0_112, <http://imagej.nih.gov/ij>) with the Open Microscopy Environment Bio-Formats library and plugin (<http://www.openmicroscopy.org/site/support/bio-formats5.4/>), allowing for the opening of Olympus files. The images were evaluated using custom colorization.

Results

Standard histological dyes for amyloid show its accumulation in human glioma tumors extracellularly and in certain tumor-related cells

Glioma tissue samples from patients of different ages (aged 35–73 years) were studied. To visualize amyloid, we used two standard histological dyes, Congo red and Th-S, known for their staining of protein amyloid aggregates. Aggregation produces a fluorescence shift, with an increase proportional to the extent of aggregation [33,34]. Coomassie brilliant blue G (BBG) was used to stain amyloid fibrils and prefibrillar amyloid intermediates [35]. We studied samples of glioma tissue (removed from four different patients: patients 17, 11, 7 and 1), and in one patient (patient 1) there were two tissue samples from the glioma zone, one containing glioma only and the other from the border zone containing glioma cells but also small fragments of normal tissue. This allowed us to use the normal tissue in the second sample as an internal reference (control). When stained with Th-S, all glioma samples examined showed a specific amyloid staining inside the tumor. In all cases, the amyloid was present in or around some glioma cells (distributed compactly or sparsely in the glioma tumor) as well as extracellularly (Fig. 1). Interestingly, the size of glioma cells stained with Th-S in samples of different patients varied by two to threefold (Fig. 1a–d).

Applying different amyloid-specific dyes, Th-S, Congo red and BBG, showed very similar staining patterns in glioma samples from patient 1, indicating the accumulation at (on or inside) some glioma cells as well as in extracellular aggregates (Fig. 1d–f). As Congo red and Th-S are known to bind only to aggregated amyloid, while BBG binds to the prefibrillar/fibrillary forms of amyloid [35], the same pattern of staining suggests that amyloid is present in glioma in both fully aggregated and pre-aggregated forms. As a control, the application of Th-S, Congo red and BBG to areas of normal tissue (Supporting information, Fig. S1a–c) showed no specific staining.

Staining with amyloid-specific dyes showed that some amyloid deposition is connected with glioma cells (accumulating on or inside the cell). This finding raises questions: which specific cells have the properties that lead to accumulation of amyloid in glioma tumors, and which type of amyloid is it? In mice, we found that glioma amyloid has A β peptide as a mandatory component and accumulates in association with GFAP-expressing glioma cells, and we suggest that this may also be the case in humans. To study this possibility we used immunostaining for human A β combined with antibodies against specific cell-type markers.

Tumor cells of glial origin and some astrocytes close to blood vessels within the tumor site accumulate A β

It is known that the main cell type in glioma tumors is malignant glioma cells of glial origin, and these have low-level but clear expression of GFAP filaments [36]. Antibodies against GFAP label glioma cells as well as astrocytes, which become reactive near the tumor, with high expression of

GFAP [37]. In addition, we recently showed that glioma cells expressing low levels of GFAP accumulate A β in mice [32]. Therefore, we decided to apply antibodies against GFAP, thereby labeling glioma cells and astrocytes, as well as an antibody specifically against NeuN, in order to distinguish between these two cell types. As mentioned above, in one patient we had two samples, one containing a highly developed glioma and another of more peripheral tissue with small insertions of normal brain tissue, allowing its use as a normal tissue reference.

To visualize A β we used two different types of antibodies highly specific for A β peptide (Figs. 2 and 3) with no cross-reaction with its precursor [38,39]. Both antibodies yielded a similar pattern of staining, showing clusters of glioma cells containing A β (Fig. 2a,d1). In addition, simultaneous application of anti-A β and anti-NeuN staining showed that cells containing A β (Fig. 2a) have no neuron-specific staining. Neuronal staining was obvious only in the sample of normal tissue as far away from the glioma as possible (Fig. 2b), and was practically non-existent in

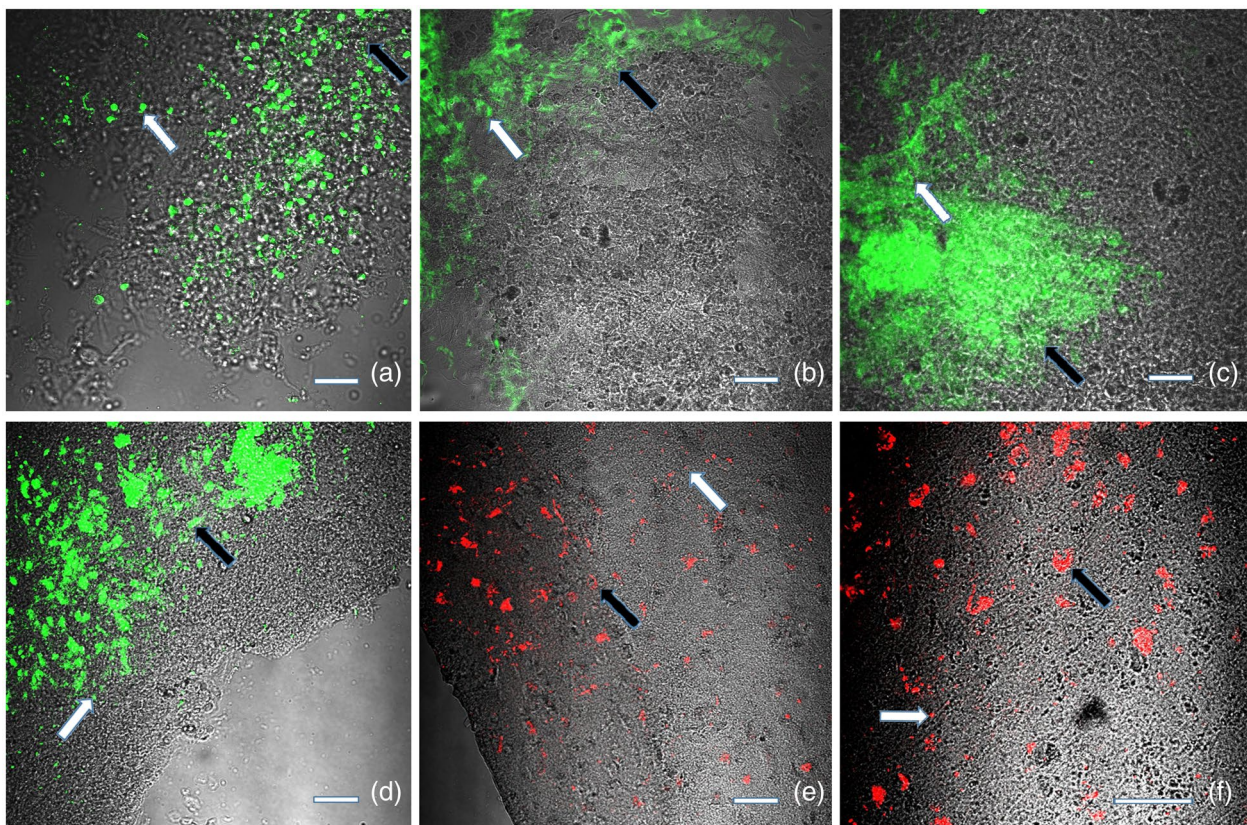


Fig. 1. Top row: glioma samples from three patients stained with thioflavin S (Th-S, green fluorescence). (a) Glioma patient 17; (b) glioma patient 11; (c) glioma patient 7. These images were acquired at the same amplification. Cells with Th-S fluorescence have different sizes in different patients. Some extracellular staining is also present, showing possible extracellular deposition. Bottom row: glioma removed from patient 1 stained with different amyloid-detecting dyes: D = thioflavin S (Th-S, green); E = Congo red (red); F = Coomassie brilliant blue G (BBG, red). All stains for amyloid beta peptides (A β) aggregates yield the same pattern of sparsely or compactly distributed cells as well as extracellular aggregates. White arrow = extracellular aggregates; black arrow = cells with amyloid; scale bar = 40 μ m.

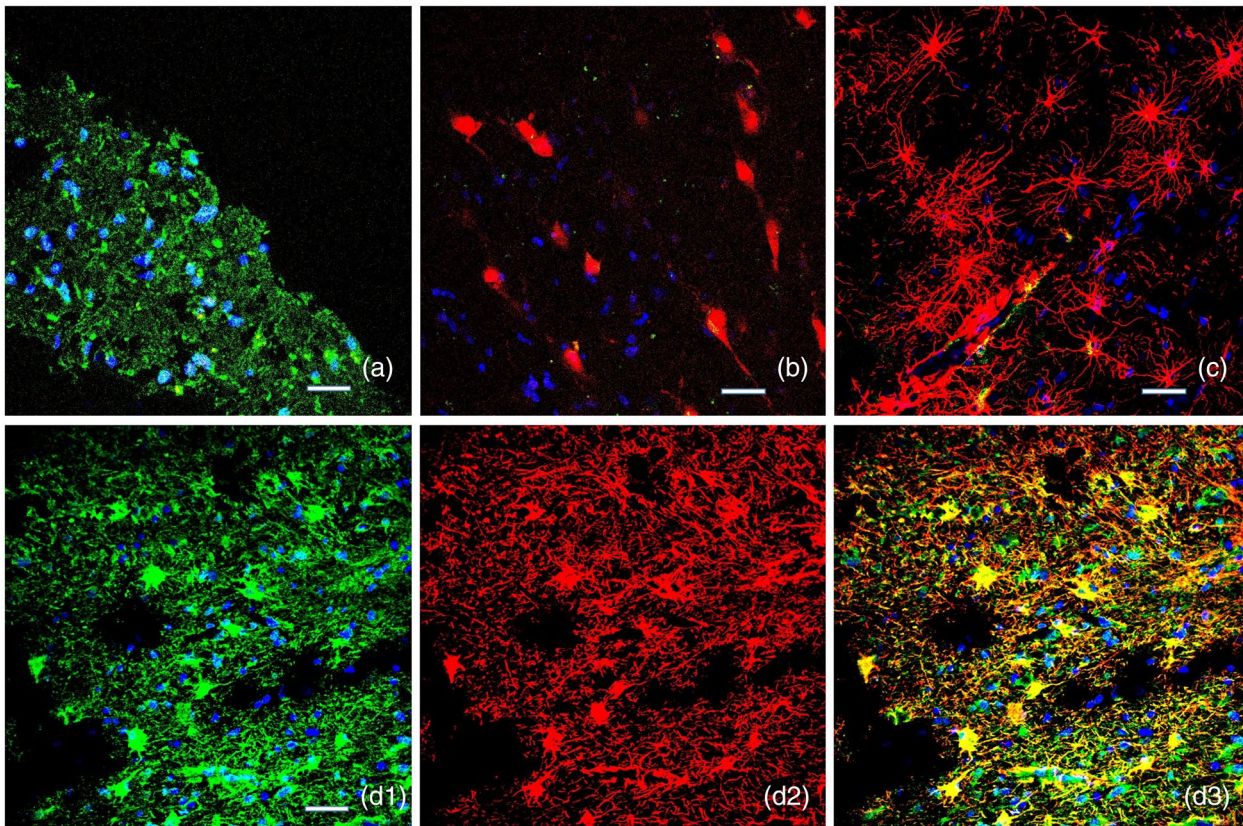


Fig. 2. Top row: double immunostaining in patient 1. (a) Compactly distributed glioma cells containing amyloid beta peptides ($A\beta$) in the main tumor (green fluorescence in cells labeled with rabbit polyclonal antibody against human $A\beta$ 1–42) double-stained with antibody against neuronal hexaribonucleotide binding protein-3 (NeuN) (red). This region contains low levels of red staining. (b) Human glioma tumor periphery (normal tissue), which contains neurons labeled with NeuN antibodies (red) but almost no anti- $A\beta$ green staining. (c) Glioma tumor periphery (normal tissue), which contains reactive astrocytes labeled with glial-specific fibrillary acidic protein (GFAP) antibodies (red), while some astrocytes sending endfeet to blood vessels have low levels of green + red = yellow staining or co-localization of glial marker anti-GFAP with anti- $A\beta$. Bottom row: in patient 1, $A\beta$ accumulates in cells of glial origin expressing GFAP. (d1) Green, polyclonal antibody against $A\beta$; blue, 4',6-diamidino-2-phenylindole (DAPI) nuclear marker; (d2) red, antibody against glial marker GFAP; (d3) composite. There is perfect co-localization of the majority of $A\beta$ -expressing cells with GFAP-expressing cells (see white arrows). Green = $A\beta$; red (in b) = NeuN (neurons); red (in c, d2, d3) = GFAP; blue (DAPI) = nuclei; scale bar, 40 μ m.

the glioma. Conversely, simultaneous application of anti- $A\beta$ and anti-GFAP staining showed that reactive astrocytes, which express GFAP, are visible on the margins of the sample containing normal tissue (Fig. 2c, upper quadrant), with no associated amyloid. This figure shows also that $A\beta$ is found in the blood vessel wall (green + red = yellow) and in some astrocytes having endfeet extending to the blood vessel wall (Fig. 2c, lower quadrant).

However, the $A\beta$ /GFAP double staining revealed that $A\beta$ accumulates mainly in cells of glial origin expressing GFAP (Fig. 2d). There was good coincidence of GFAP-expressing cells (Fig. 2d1, red) and $A\beta$ -containing cells (Fig. 2d2, green, also Fig. 2d3, composite). These cells have much less arborization than astrocytes and sometimes less pronounced GFAP expression in the cell body (Fig. 2d2). The majority of these GFAP-expressing cells

have associated amyloid, although it is difficult to ascertain whether there is also extracellular amyloid present.

Amyloid in glioma cells is mainly present in cells around blood vessels and in perivascular spaces

It is known that glioma is highly vascular, and tumor invasion along blood vessels facilitates its spread in the brain [40]. Similarly, we found that there is a substantial accumulation of $A\beta$ in blood vessel walls and in the cells around blood vessels (Fig. 3a–c). Green fluorescence of Congo red (FITC filter) at low magnification (Fig. 3a) shows that amyloid aggregates mainly in cells around and inside the blood vessels. The red fluorescence of Congo red (TRITC filter) enables visualization of blood vessel walls in general, because this non-specific red fluorescence stain labels mainly the vessel walls [41]. A very similar result was found by

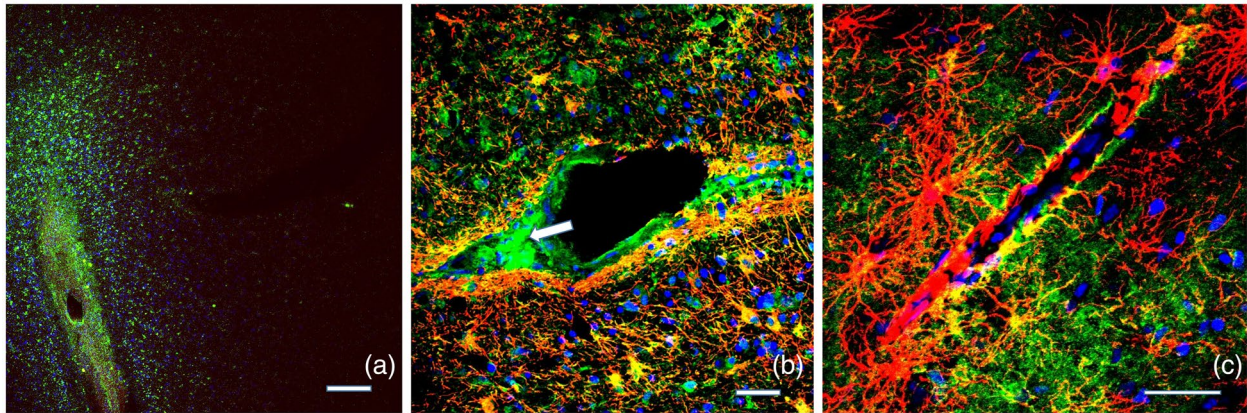


Fig. 3. Amyloid around blood vessels in glioma. (a) Congo red staining of amyloid (green) at low magnification ($\times 10$) showing amyloid-containing cells concentrated around the large blood vessel (red), on the inner surface of the vessel and in the perivascular space. (b) Anti-amyloid beta peptides ($A\beta$) antibody (green) shows that $A\beta$ -containing cells are co-localized with glial-specific fibrillary acidic protein (GFAP) (red)-containing cells of glial origin around blood vessels. Some $A\beta$ -containing cells are present at the inner surface of the blood vessel wall and in the perivascular space, and these cells do not always coincide with GFAP. (c) $A\beta$ -containing cells (green) around small blood vessels in samples containing normal tissue. Some reactive astrocytes in the layer on top of the glioma cell layer had started to accumulate amyloid. $A\beta$ is found in the blood vessel walls and in the astrocytic endfeet on the vessel walls (green + red = yellow). Arrow in B = perivascular space; blue = 4',6-diamidino-2-phenylindole (DAPI) staining (nuclei). Scale bars = 240 μm ; (a) 40 μm (b,c).

immunostaining with an antibody against $A\beta$ (green), which is concentrated in glioma cells around the blood vessels but especially in the vessel walls and in the perivascular space (Fig. 3b, arrow). In a marginal sample (Fig. 3c) there was a layer of normal reactive astrocytes (red) lying on top of the glioma cell layer (green). In this figure (Fig. 3c), $A\beta$ fluorescence is also present in the blood vessel walls and in the endfeet of astrocytes on the surface of the vessels. We also present this figure as a series of confocal images to clarify the three-dimensional positions of different cell layers (Supporting information, Fig. S2).

Discussion

Recently, we found that glioma in mice accumulate $A\beta$, mainly in glioma cells expressing GFAP and around nearby blood vessels [32]. We suggested that the amyloid in this tumor might be used as a target to develop a novel class of drugs for visualization and treatment of glioma. This possibility has inspired us to determine whether a similar accumulation is found in human glioma.

Here we report that amyloid-specific dyes (Th-S, Congo red, BBG) show amyloid accumulation in all human glioma samples that we received from different patients. Some amyloid was present extracellularly, but was mainly concentrated in glioma cells (Fig. 1). Application of two different antibodies against $A\beta$ peptide (a polyclonal antibody against human $A\beta_{1-42}$ and a monoclonal pan-specific mAb-2 antibody against $A\beta$ residues 1–4) revealed that the amyloid

in glioma samples contains $A\beta$ and that both antibodies show a similar staining pattern (compare Fig. 2a with Fig. 2d1). Double staining with antibodies to cell-specific antigens showed that $A\beta$ accumulation is present mainly in glioma cells of glial origin that express GFAP, in blood vessel walls and in some astrocytes close to the glioma body. No correlation between $A\beta$ and a specific neuronal marker was found (Fig. 2b). These results fully support our previous study in a mouse model of glioma [32].

Our decision to first investigate neurons and astrocytes as possible sources of $A\beta$ was motivated by the fact that these cell types are known for their ability to produce large amounts of $A\beta$ peptide [42,43]. It was previously shown that astrocytes may also take up $A\beta$ generated by other cell types [44]. We also suspected glioma cells, as the production of $A\beta$ by cultured malignant glioma cells was shown: these cells produce a 4-kDa peptide that co-migrates with synthetic $A\beta_{1-40}$ (also known as $A\beta_{40}$) and is specifically recognized by antibodies raised against terminal domains of the $A\beta$ peptide, and the cells release this peptide into the medium [45]. These results and our previous experience with a mouse glioma model allow us to suggest which types of cells are involved. There are many other cell types associated with glioma; for example, myeloid-derived suppressor cells (MDSCs), regulatory T cells and tumor-associated macrophages (TAMs) [46], as well as microglia [47], but their presence is stage-dependent, and they constitute a smaller population of cells. Therefore, we decided to first study neuronal/glial markers and return to other

cells if these markers failed to reveal which cells accumulate amyloid. This approach was successful in confirming that GFAP-expressing glioma cells of glial origin show A β fluorescence (Figs. 2a and 2d1), as do some astrocytes (Fig. 2d3) and the blood vessel walls (Fig. 3). This result may be interpreted in different ways: either (1) glioma cells produce A β or (2) A β is produced systemically and migrates to glioma. This last possibility can explain why amyloid is concentrated around blood vessels (Fig. 3a,b).

Interestingly, statistically independent cohort studies found an inverse association between cancers in general and Alzheimer's disease (AD) [48,49]. Nevertheless, there is a significant positive correlation between AD and the malignant brain tumor mortality rate, suggesting that there are common mechanisms [50–52]. Could it be that a common systemic source of A β production is involved?

While glioma cells produce A β , its production is very limited [45]. Systemic production of A β is also well known, and recently we showed that platelets produce a massive release of A β after thrombosis in the brain or skin and that this release is concentrated near blood vessels [39,53]. A β was shown to be an anti-microbial/anti-viral agent and the important part of the systemic innate immunity arsenal [29,54–59]. We also previously suggested that blood platelet activation, as a response to the inflammation, can add to the accumulation of A β in AD (reviewed in [19]). It was shown that platelets become hyperactivated in AD [60], and this may lead to excessive release of A β in the brain, overwhelming its clearance during the disease. A similar accumulation of A β happens during glaucoma, in damaged skin and during pre-eclampsia [20].

It has also been shown that platelets are hyperactivated in cancer patients and form cancer cell-induced aggregates and micro-thrombi in the vasculature near tumors (reviewed in [61]). We suggest that these platelet aggregates can release A β . Release of systemic A β peptides may also be a response to the development of glioma in the brain and even a weapon against glioma. It was reported that full-length A β 40 and its shorter fragments suppress human U87 glioblastoma subcutaneous xenografts in nude mice, while systemic delivery of this shorter peptide leads to reductions in glioma proliferation, angiogenesis and invasiveness [62]. The same investigators also found that transgenic mice over-expressing A β 40 showed reductions in glioma growth, invasion and angiogenesis [63,64]. Recently, there has been another report that A β oligomers are an effective weapon against cancer cells [31]. The mechanism of external A β accumulation in glioma cells expressing GFAP may also be because of modified RAGE (a receptor for A β) isoform expression on their surface and not only in

tumor-associated macrophages [65,66]. Generally, high platelet count is associated with poor survival in a large variety of cancers, while thrombocytopenia or anti-platelet drugs can reduce the short-term risk of cancer, cancer mortality and metastasis (reviewed in [67]).

Conclusions

It is now clear that A β -containing amyloid in glioma is an obligatory part of the tumor environment, although it is still uncertain whether A β build-up is a systemic innate immunity reaction to the tumor, or A β peptides are produced locally by glioma cells. Aggregated amyloid and amyloid intermediates were present inside glioma tumors of all studied glioma samples, while A β peptide immunofluorescence labeled glioma cells, nearby astrocytes and blood vessels. In any case, A β peptides and their amyloid aggregates are highly specific antigens, and their presence in glioma tumors can be used to mark glioma cells for visualization, as there are many substances already approved by the Food and Drug Administration for this purpose [68]. The amyloid build-up in glioma tumors may also be used as a target to develop a novel class of anti-tumor drugs.

Acknowledgements

We would like to thank Dr L. Kucheryavykh and the personnel of her laboratory in Universidad Central del Caribe for their kind help. This research was supported by NIH grants SC2GM111149 to M. I. The funding sources had no role in study design; data collection, analysis or interpretation; or the decision to submit this article.

Disclosures

The authors declare that they have no conflicts of interest.

Author contributions

A. Z.-S. performed experiments, analysed the data, and cowrote the paper; A. D.-G. performed experiments, analyzed the data and co-wrote the paper; R. N.-R. performed experiments and analyzed the data; M. I. designed the study, analyzed the data and co-wrote the paper.

References

- 1 Cohen AD, Zhou P, Xiao Q *et al.* Systemic AL amyloidosis due to non-Hodgkin's lymphoma: an unusual clinicopathologic association. *Br J Haematol* 2004; **124**:309–14.
- 2 Gertz MA, Merlini G, Treon SP. Amyloidosis and Waldenström's macroglobulinemia. *Hematol Am Soc Hematol Educ Program* 2004:257–82.

- 3 Bahlis NJ, Lazarus HM. Multiple myeloma-associated AL amyloidosis: is a distinctive therapeutic approach warranted? *Bone Marrow Transplant* 2006; **38**:7–15.
- 4 Suzuki K. Diagnosis and treatment of multiple myeloma and AL amyloidosis with focus on improvement of renal lesion. *Clin Exp Nephrol* 2012;**16**:659–71.
- 5 Silverman JF, Dabbs DJ, Norris HT, Pories WJ, Legier J, Kay S. Localized primary (AL) amyloid tumor of the breast. Cytologic, histologic, immunocytochemical and ultrastructural observations. *Am J Surg Pathol* 1986; **10**:539–45.
- 6 Mori M, Kotani H, Sawaki M *et al.* Amyloid tumor of the breast. *Surg Case Rep* 2019; 5:31.
- 7 Valenta LJ, Michel-Bechet M, Mattson JC, Singer FR. Microfollicular thyroid carcinoma with amyloid rich stroma, resembling the medullary carcinoma of the thyroid (MCT). *Cancer* 1977; **39**:1573–86.
- 8 Khan IS, Loh KS, Petersson F. Amyloid and hyaline globules in undifferentiated nasopharyngeal carcinoma. *Ann Diagn Pathol* 2019; **40**:1–6.
- 9 Rosenzweig M, Landau H. Light chain (AL) amyloidosis: update on diagnosis and management. *J Hematol Oncol* 2011; **4**:47.
- 10 Okamoto S, Togo S, Nagata I *et al.* Lung adenocarcinoma expressing receptor for advanced glycation end-products with primary systemic AL amyloidosis: a case report and literature review. *BMC Cancer* 2017; **17**:22.
- 11 Stewart KL, Radford SE. Amyloid plaques beyond A β : a survey of the diverse modulators of amyloid aggregation. *Biophys Rev* 2017; **9**:405–19.
- 12 Chaudhuri P, Prajapati KP, Anand BG, Dubey K, Kar K. Amyloid cross-seeding raises new dimensions to understanding of amyloidogenesis mechanism. *Ageing Res Rev* 2019; **56**:100937.
- 13 Köppen J, Schulze A, Machner L *et al.* Amyloid-beta peptides trigger aggregation of alpha-synuclein *in vitro*. *Molecules* 2020; **25**:pii:E580.
- 14 NIH. Tumor Markers. NIH National Cancer Institute. Available at: <https://www.cancer.gov/about-cancer/diagnosis-staging/diagnosis/tumor-markers-fact-sheet> (accessed 2/10/20).
- 15 Franklin CD, Martin MV, Clark A, Smith CJ, Hindle MO. An investigation into the origin and nature of ‘amyloid’ in a calcifying epithelial odontogenic tumour. *J. Oral Pathol* 1981; **10**:417–29.
- 16 Delaney MA, Singh K, Murphy CL, Solomon A, Nel S, Boy SC. Immunohistochemical and biochemical evidence of ameloblastic origin of amyloid-producing odontogenic tumors in cats. *Vet Pathol* 2013; **50**:238–42.
- 17 Hirayama K, Endoh C, Kagawa Y *et al.* Amyloid-producing odontogenic tumors of the facial skin in three cats. *Vet Pathol* 2017; **54**:218–21.
- 18 McCarthy E. Amyloidosis in bone. In: Santini-Araujo E, Kalil R, Bertoni F, Park YK, eds. *Tumors and Tumor-Like Lesions of Bone*. London: Springer; 2015:933–937.
- 19 Inyushin MY, Sanabria P, Rojas L, Kucheryavykh Y, Kucheryavykh L. A β peptide originated from platelets promises new strategy in anti-Alzheimer’s drug development. *Biomed Res Int* 2017; **2017**:3948360.
- 20 Inyushin M, Zayas-Santiago A, Rojas L, Kucheryavykh Y, Kucheryavykh L. Platelet-generated amyloid beta peptides in Alzheimer’s disease and glaucoma. *Histol Histopathol* 2019; **32**:843–56.
- 21 Jin WS, Bu XL, Liu YH *et al.* Plasma amyloid-beta levels in patients with different types of cancer. *Neurotox Res* 2017; **31**:283–8.
- 22 Nolte I, Przibylla H, Bostel T, Groden C, Brockmann MA. Tumor-platelet interactions: glioblastoma growth is accompanied by increasing platelet counts. *Clin Neurol Neurosurg* 2008; **110**:339–42.
- 23 Marx S, Xiao Y, Baschin M *et al.* The role of platelets in cancer pathophysiology: focus on malignant glioma. *Cancers* 2019; **11**:569.
- 24 Chen M, Inestrosa CC, Ross GS, Fernandez HL. Platelets are the primary source of amyloid P-peptide in human blood. *Biochem Biophys Res Commun* 1995; **213**:96–103.
- 25 Humpel C. Platelets: their potential contribution to the generation of beta-amyloid plaques in Alzheimer’s disease. *Curr Neurovasc Res* 2017; **14**:290–8.
- 26 Horstman LL, Jy W, Ahn YS *et al.* Role of platelets in neuroinflammation: a wide-angle perspective. *J Neuroinflammation* 2010; **7**:10.
- 27 Sotnikov I, Veremeyko T, Starossom SC, Barteneva N, Weiner HL, Ponomarev ED. Platelets recognize brain-specific glycolipid structures, respond to neurovascular damage and promote neuroinflammation. *PLOS ONE* 2013; **8**:e58979 [published correction appears in *PLOS ONE* 2014 Jan 8;9(1):null].
- 28 Ali RA, Wuescher LM, Worth RG. Platelets: essential components of the immune system. *Curr Trends Immunol* 2015; **16**:65–78.
- 29 Eriksson O, Mohlin C, Nilsson B, Ekdahl KN. The human platelet as an innate immune cell: interactions between activated platelets and the complement system. *Front Immunol* 2019; **10**:1590.
- 30 Brothers HM, Gosztyla ML, Robinson SR. The physiological roles of amyloid- β peptide hint at new ways to treat Alzheimer’s disease. *Front Aging Neurosci* 2018; **10**:118.
- 31 Pavliukeviciene B, Zentelyte A, Jankunec M *et al.* Amyloid β oligomers inhibit growth of human cancer cells. *PLOS ONE* 2019; **14**:e0221563.
- 32 Kucheryavykh LY, Ortiz-Rivera J, Kucheryavykh YV, Zayas-Santiago A, Diaz-Garcia A, Inyushin MY. Accumulation of innate amyloid beta peptide in glioblastoma tumors. *Int J Mol Sci* 2019; **20**. pii: E2482.
- 33 Rajamohamedsait HB, Sigurdsson EM. Histological staining of amyloid and pre-amyloid peptides and proteins in mouse tissue. *Methods Mol Biol* 2012; **849**:411–24.
- 34 Yakupova EI, Bobyleva LG, Vikhlyantsev IM. Congo Red and amyloids: history and relationship. *Biosci Rep* 2019; **39**. pii: BSR20181415.

- 35 Wong HE, Qi W, Choi HM, Fernandez EJ, Kwon I. A safe, blood-brain barrier permeable triphenylmethane dye inhibits amyloid- β neurotoxicity by generating nontoxic aggregates. *ACS Chem Neurosci* 2011; **2**:645–57.
- 36 Gullotta F, Schindler F, Schmutzler R, Weeks-Seifert A. GFAP in brain tumor diagnosis: possibilities and limitations. *Pathol Res Pract* 1985; **180**:54–60.
- 37 Kucheryavykh LY, Rolón-Reyes K, Kucheryavykh YV *et al.* Glioblastoma development in mouse brain: general reduction of OCTs and mislocalization of OCT3 transporter and subsequent uptake of ASP+ substrate to the nuclei. *J Neurosci Neuroeng* 2014; **3**:3–9.
- 38 Youmans KL, Tai LM, Kanekiyo T *et al.* Intraneuronal A β detection in 5xFAD mice by a new A β -specific antibody. *Mol Neurodegener* 2012; **7**:8.
- 39 Kucheryavykh LY, Dávila-Rodríguez J, Rivera-Aponte DE *et al.* Platelets are responsible for the accumulation of β -amyloid in blood clots inside and around blood vessels in mouse brain after thrombosis. *Brain Res Bull* 2017; **128**:98–105.
- 40 Watkins S, Robel S, Kimbrough IF, Robert SM, Ellis-Davies G, Sontheimer H. Disruption of astrocyte–vascular coupling and the blood–brain barrier by invading glioma cells. *Nat Commun* 2014; **19**:4196.
- 41 Linke RP. Congo Red staining of amyloid: improvements and practical guide for a more precise diagnosis of amyloid and the different amyloidosis. In: Uversky VN, Fink AL, eds. *Protein Misfolding, Aggregation, and Conformational Diseases*. Protein Reviews, vol 4. Boston, MA: Springer; 2006: 239–76.
- 42 Cras P, Kawai M, Siedlak S *et al.* Neuronal and microglial involvement in beta-amyloid protein deposition in Alzheimer's disease. *Am J Pathol* 1990; **137**:241–6.
- 43 Zhao J, O'Connor T, Vassar R. The contribution of activated astrocytes to A β production: implications for Alzheimer's disease pathogenesis. *J Neuroinflammation* 2011; **8**:150.
- 44 Söllvander S, Nikitidou E, Brolin R, *et al.* Accumulation of amyloid- β by astrocytes result in enlarged endosomes and microvesicle-induced apoptosis of neurons. *Mol Neurodegener* 2016; **11**:38.
- 45 Morato E, Mayor F Jr. Production of the Alzheimer's beta-amyloid peptide by C6 glioma cells. *FEBS Lett* 1993; **336**:275–8.
- 46 Kamran N, Kadiyala P, Saxena M *et al.* Immunosuppressive myeloid cells' blockade in the glioma microenvironment enhances the efficacy of immune-stimulatory gene therapy. *Mol Ther* 2017; **25**:232–48.
- 47 Rolón-Reyes K, Kucheryavykh YV, Cubano LA *et al.* Microglia activate migration of glioma cells through a Pyk2 intracellular pathway. *PLOS ONE* 2015; **10**:e0131059.
- 48 Ou SM, Lee YJ, Hu YW *et al.* Does Alzheimer's disease protect against cancers? A nationwide population-based study. *Neuroepidemiology* 2013; **40**:42–9.
- 49 Musicco M, Adorni F, Di Santo S *et al.* Inverse occurrence of cancer and Alzheimer disease: a population-based incidence study. *Neurology* 2013; **81**:322–8.
- 50 Behrens MI, Lendon C, Roe CM. A common biological mechanism in cancer and Alzheimer's disease? *Curr Alzheimer Res* 2009; **6**:196–204.
- 51 Lehrer S. Glioblastoma and dementia may share a common cause. *Med Hypotheses* 2010; **75**:67–8.
- 52 Sánchez-Valle J, Tejero H, Ibáñez K *et al.* A molecular hypothesis to explain direct and inverse co-morbidities between Alzheimer's disease, glioblastoma and lung cancer. *Sci Rep* 2017; **7**:4474.
- 53 Kucheryavykh LY, Kucheryavykh YV, Washington AV, Inyushin MY. Amyloid beta peptide is released during thrombosis in the skin. *Int J Mol Sci* 2018; **19**:1705.
- 54 Lukiw WJ, Cui JG, Yuan LY *et al.* Acyclovir or A β 42 peptides attenuate HSV-1-induced miRNA-146a levels in human primary brain cells. *Neuroreport* 2010; **21**:922–7.
- 55 Soscia SJ, Kirby JE, Washicosky KJ *et al.* The Alzheimer's disease-associated amyloid beta-protein is an antimicrobial peptide. *PLOS ONE* 2010; **5**:e9505.
- 56 Bourgade K, Garneau H, Giroux G *et al.* β -Amyloid peptides display protective activity against the human Alzheimer's disease-associated herpes simplex virus-1. *Biogerontology* 2015; **16**:85–98.
- 57 White MR, Kandel R, Tripathi S *et al.* Alzheimer's associated β -amyloid protein inhibits influenza A virus and modulates viral interactions with phagocytes. *PLOS ONE* 2014; **9**:e101364.
- 58 Kumar DK, Choi SH, Washicosky KJ *et al.* Amyloid- β peptide protects against microbial infection in mouse and worm models of Alzheimer's disease. *Sci Transl Med* 2016; **8**:340ra72.
- 59 Gosztyla ML, Brothers HM, Robinson SR. Alzheimer's amyloid- β is an antimicrobial peptide: a review of the evidence. *J Alzheimers Dis* 2018; **62**:1495–506.
- 60 Sevush S, Jy W, Horstman LL, Mao WW, Kolodny L, Ahn YS. Platelet activation in Alzheimer disease. *Arch Neurol* 1998; **55**:530–6.
- 61 Jurasz P, Alonso-Escolano D, Radomski MW. Platelet–cancer interactions: Mechanisms and pharmacology of tumour cell-induced platelet aggregation. *Br J Pharm* 2004; **143**:819–26.
- 62 Murphy SF, Banasiak M, Yee G-T *et al.* A synthetic fragment of beta-amyloid peptide suppresses glioma proliferation, angiogenesis, and invasiveness *in vivo* and *in vitro*. *Neuro-Oncol* 2010; **12**:iv5.
- 63 Paris D, Ganey N, Banasiak M *et al.* Impaired orthotopic glioma growth and vascularization in transgenic mouse models of Alzheimer's disease. *J. Neurosci* 2010; **30**:11251–8.
- 64 Paris D. Modulation of Angiogenesis by a-Beta Peptide Fragments. Patent US20080031954A1, 7 February 2005. Available at: <https://patents.google.com/patent/US20080031954> (accesses 7/30/2020).
- 65 Jules J, Maignel D, Hudson BI. Alternative splicing of the RAGE cytoplasmic domain regulates cell signaling and function. *PLOS ONE* 2013; **8**:e78267.
- 66 Tekabe Y, Johnson J, Li Q *et al.* Molecular imaging of RAGE expression in human glioblastoma. *Clin Oncol* 2019; **4**:1609.
- 67 Goubran HA, Burnouf T, Radosevic M, El-Ekiaby M. The platelet–cancer loop. *Eur J Intern Med* 2013; **24**:393–400.
- 68 Barthel H, Sabri O. Clinical use and utility of amyloid imaging. *J Nucl Med* 2017; **58**:1711–7.

Supporting Information

Additional Supporting Information may be found in the online version of this article at the publisher's web site:

Fig. S1. Samples of glioma with peripheral (control) tissue removed from Patient 1 and stained with different

amyloid-detecting dyes: A, thioflavin S (Th-S, green); B, Congo red (red); C, Coomassie brilliant blue G (BBG, red). These slices show no visible staining. Scale bar, 40 μm .

Fig. S2. see <https://inyushinlab.org/accumulation-of-amyloid-beta-in-human-glioblastomas/>